Photoassembly of the manganese cluster and oxygen evolution from monomeric and dimeric CP47 reaction center photosystem II complexes

Claudia Büchel*, Jim Barber*†, Gennady Ananyev‡, Said Eshaghi*, Richard Watt‡, and Charles Dismukes‡

*Biochemistry Department, Imperial College of Science, Technology and Medicine, London SW7 2AY, United Kingdom; and ‡Department of Chemistry, Hoyt Laboratory, Princeton University, Princeton, NJ 08544

Edited by Johann Deisenhofer, University of Texas Southwestern Medical Center, Dallas, TX, and approved October 18, 1999 (received for review June 28, 1999)

Isolated subcomplexes of photosystem II from spinach (CP47RC), composed of D1, D2, cytochrome b_{559}, CP47, and a number of hydrophobic small subunits but devoid of CP43 and the extrinsic proteins of the oxygen-evolving complex, were shown to reconstitute the $Mn_4Ca_1Cl_x$ cluster of the water-splitting system and to evolve oxygen. The photoactivation process in CP47RC dimers proceeds by the same two-step mechanism as observed in PSII membranes and exhibits the same stoichiometry for Mn^{2+}, but with a 10-fold lower affinity for Ca^{2+} and an increased susceptibility to photodamage. After the lower Ca^{2+} affinity and the 10-fold smaller absorption cross-section for photons in CP47 dimers is taken into account, the intrinsic rate constant for the rate-limiting calcium-dependent dark step is indistinguishable for the two systems. The monomeric form of CP47RC also showed capacity to photoactivate and catalyze water oxidation, but with lower activity than the dimeric form and increased susceptibility to photodamage. After optimization of the various parameters affecting the photoactivation process in dimeric CP47RC subcores, 18% of the complexes were functionally reconstituted and the quantum efficiency for oxygen production by reactivated centers approached 96% of that observed for reconstituted photosystem II-enriched membranes.

Green plants, algae, and cyanobacteria are unique in their ability to catalyze the oxidation of water to molecular oxygen by using light energy. This process is carried out by photosystem II (PSII), a protein complex embedded in the thylakoid membrane. It consists of more than 25 different subunits, binds a large number of pigments, and contains a photochemical reaction center for light-driven charge separation (see recent reviews in refs. 1–5). In this paper we show that oxygen evolution is possible from a subcomplex composed of a small number of these subunits after reconstituting the catalytic inorganic center.

The innermost part of PSII consists of the reaction center (RC), which, when isolated, is composed of the D1 and D2 proteins, where the primary charge separation occurs, the *psbI* gene product, and the α- and β-subunits of cytochrome b_{559} (6). Closely associated with the RC are the chlorophyll- and β-carotene-binding "inner antenna" proteins CP43 and CP47 and a range of small, hydrophobic polypeptides, which, together, comprise the PSII core complex. Several of these subunits have been proposed to contain residues essential for water oxidation.

Water oxidation occurs at a catalytic site containing a tetramanganese cluster, one calcium ion, and an indeterminate number of chloride ions in association with tyrosyl residue Tyr161 (Y_Z) located in the D1 protein. Evidence to date indicates that the majority of ligands binding the manganese cluster are located in the D1 protein (7–10). The oxidized tyrosyl radical Y_Z· is reduced by electrons from the manganese cluster after being oxidized by the light-driven charge separation. This charge separation involves the oxidation of the primary electron donor P680 and reduction of the tightly bound plastoquinone acceptor, Q_A. The D1/D2-heterodimer is bordered by the CP47 and CP43 inner antenna proteins, which have extremely large luminal loops that also could play a role in stabilizing the $Mn_4Ca_1Cl_xY_z$ site (11, 12). Despite all efforts, the exact spatial location and detailed geometry of the four manganese atoms remain controversial. The several models proposed have been reviewed (13–15). In eukaryotic organisms the $Mn_4Ca_1Cl_xY_z$ site is protected from inadvertent reduction by diffusable components located in the thylakoid lumen by three extrinsic proteins with molecular masses of 33 kDa, 23 kDa, and 17 kDa (16). These proteins along with CP47/CP43 also appear to function in concentrating the levels of Cl^- and/or Ca^{2+} at the catalytic site of water oxidation (1, 11).

One of the most astonishing features is the way the manganese cluster self-assembles. Unlike other inorganic metal clusters observed in nature that undergo spontaneous self-assembly or require accessory, chaperonin-like proteins for proper formation, the tetramanganese cluster is assembled by a light-driven reaction called photoactivation (17). This photoactivation requires weak light, Mn^{2+}, Ca^{2+}, and Cl^- (18, 19). The assembly of the Mn cluster in PSII-enriched membranes was found to be minimally a two-step process requiring an essential dark process in between light-dependent steps (19, 20). In a recent extension of this approach, the first two kinetic steps in the photoactivation process were resolved as summarized in Scheme 1 (21–24). According to this scheme, Mn^{2+} binds as $Mn(OH)^+$ to a high-affinity site, is subsequently oxidized to $Mn(OH)^{2+}$ in the first light-dependent reaction, and, after releasing a proton, forms the first intermediate, $Mn(OH)_2^+$ (IM_1). In the dark period that follows, one Ca^{2+} must bind at its effector site so that stable binding and photooxidation of the second (and subsequent) Mn^{2+} can occur during the next photolytic event and so generate the second intermediate (IM_2). This dark, calcium-dependent process is the rate-limiting step of photoactivation. The binding of the remaining two Mn^{2+} occurs via a cooperative process that has not been resolved kinetically (19, 20, 25).

All of the photoactivation studies reported to date have been performed by using PSII cores (26), PSII membranes (19, 20), or larger, native-like preparation (18, 27, 28). The possibility of oxygen evolution from smaller PSII subcore complexes has not been demonstrated previously, although Rögner *et al.* (29) had shown that a PSII complex can form within the photosynthetic membrane in a CP43 deletion mutant of *Synechocystis* that

This paper was submitted directly (Track II) to the PNAS office.

Abbreviations: Chl, chlorophyll; DCBQ, dichloro-benzoquinone; ferricyanide, $K_3Fe(CN)_6$; PSII, photosystem II; Q_A, primary plastoquinone acceptor of PSII; RC, reaction center of photosystem II; t_{dark}, dark time between flashes; WOC, water oxidizing complex; t_{lag}, lag time parameter.

†To whom reprint requests should be addressed. E-mail j.barber@ic.ac.uk.

The publication costs of this article were defrayed in part by page charge payment. This article must therefore be hereby marked "*advertisement*" in accordance with 18 U.S.C. §1734 solely to indicate this fact.

supported electron transfer between Y_Z and the first plastoquinone acceptor, Q_A, but not O_2 evolution. Their results suggested to us that it may be possible to photoactivate the CP47RC subcomplex *in vitro*.

Recently, a PSII subcore complex lacking CP43 and the three extrinsic proteins but containing CP47 as well as the reaction center (CP47RC) has been isolated in both monomeric and dimeric forms (30), and their electron transport properties have been characterized (31). In this work we show that the CP47RC dimers as well as the monomers can be photoactivated, i.e., reassembling the $Mn_4Ca_1Cl_x$ cluster and evolving oxygen with a high degree of conversion. This result opens up new discussions about the minimal structural unit required for oxygen evolution.

Materials and Methods

Isolation of CP47RC Complexes. CP47RC complexes were purified according to the method described in Zheleva *et al.* (30): PSII-enriched membranes (32) were obtained from market spinach and frozen until use. To remove the extrinsic proteins, PSII-enriched membranes were washed in 0.2 M Tris, pH 9. Samples were solubilized by using 2.7% heptyl-glucopyranoside and 1% β-dodecyl maltoside and loaded on an anion-exchange column (DEAE Toyopearl 650S, TSK) by using 50 mM Tris, pH 7.3, as buffer and only β-dodecyl maltoside as detergent. After intensive washing to remove all light-harvesting proteins and CP43, crude CP47RC complexes were eluted. Further separation into CP47RC monomers and dimers was carried out by sucrose density centrifugation. Samples were concentrated, frozen in liquid nitrogen, and stored at −80°C until use.

Characterization of the CP47RC Complexes Used for Photoactivation. The CP47RC preparations were checked for their purity by recording their absorption spectra, protein composition, and aggregation state (monomeric or dimeric). Absorption spectra and SDS/PAGE were carried out as described in Zheleva *et al.* (30). The aggregation state was confirmed by using size-exclusion HPLC (30). To test for any contamination by core complexes as judged by the presence of CP43, monomers as well as dimers were run on a SDS-polyacrylamide gel and Western blots were performed by using a spinach CP43 antibody and visualized by luciferase assay (enhanced chemiluminescence; Amersham Pharmacia). To quantify the contamination, a dilution series of CP43 purified according to Büchel *et al.* (33) was blotted in parallel. The CP43 antibody was a kind gift from Roberto Barbato, Padova. By loading CP47RC complexes in the nanomolar and CP43 in the picomolar range, no CP43 contamination could be found in the case of the monomers. In the case of the dimers, a very low level of CP43 was detected, estimated from the serial dilutions to be 3.75 pmol CP43 in 1.3 nmol CP47RC dimer complexes, i.e., 0.3% contamination (Fig. 1).

Fluorescence yield changes under continuous illumination (F_v) in comparison with the constant fluorescence (F_o) induced by the nonactinic measuring beam alone were used to check for photoreducible Q_A according to Bianchetti *et al.* (31). As described earlier, the dimers showed variable fluorescence because of their Q_A content, whereas the monomers were free of any photoreducible quinone.

Photoactivation and Oxygen Yield Measurements. Photoactivation and amperometric detection of oxygen on a membrane-coated electrode were performed directly by using a home-built microcell (volume 5 μl) at 25°C as described earlier (21, 22). The current signal was amplified in a two-stage band-pass-filtered amplifier (0.3–3.0 Hz), yielding a sensitivity of 50 fmol O_2 at a time constant of 0.1 s. Signals were either recorded directly or sent via an analogue-to-digital converter (WINDAQ) to a computer. Illumination of the samples on the membrane/electrode was carried out by using an ultrabright LED with a wavelength maximum of 660 nm and a peak intensity of 800 mW/cm^2 (HLMP-8102; Hewlett Packard), providing illumination times in the range from 1 ms to continuous illumination. Illumination and data acquisition were controlled by a computer program (LABVIEW) that allows different flash lengths and dark times (t_{dark}) between the flashes. The light regime in the different experiments is given in the text or the figure legends.

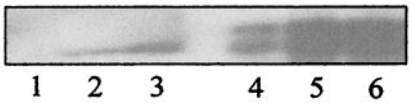

Fig. 1. Immunoblot using CP43 antibody to calculate contamination with CP43 in the CP47RC monomers and dimers. Loading was based on molar levels of the complexes. Lanes: 1, CP47RC monomer, 0.74 nmol; 2, CP47RC dimer, 0.67 nmol; 3, CP47RC dimer, 1.3 nmol; 4, CP43, 7.5 pmol; 5, CP43, 35 pmol; 6, CP43, 75 pmol. Using lanes 4–6 for a calibration curve, the CP43 contamination corresponds to 1.88 pmol in 0.67 nmol CP47RC dimers (lane 2) and 3.75 pmol in 1.3 nmol CP47RC dimers (lane 3), i.e., 0.3% contamination.

For each photoactivation experiment, CP47RC complexes were used at a concentration equivalent to 10 μM RCs, based on the known chlorophyll content taking into account 21 or 19 chlorophyll (Chl)/2 pheophytin as estimated by reversed-phase HPLC for dimers and monomers, respectively (30). The final concentration of the sample buffer was 50 mM Mes, pH 6.0/25 mM NaCl/0.3 M sucrose. All measurements were carried out by using 0.8 mM $K_3Fe(CN)_6$ (ferricyanide) as an electron acceptor. Ferricyanide, $MnCl_2$, and $CaCl_2$ at the concentrations given in the text or figure legends were added 10 min before illumination began during an initial dark incubation. For comparison of the maximal oxygen evolution capacity, PSII-enriched membranes were depleted in manganese and calcium by treatment with 25 mM chelator tetrapropionato-1,3-di(amino-methyl)benzene as described previously (21, 22) and photoactivated by using optimal salt, light, and acceptor conditions. This procedure photoactivates >99% of all centers (21). These treated PSII membranes are also depleted of the extrinsic proteins and are referred to as apo-WOC-PSII membranes in this paper.

Results

CP47RC dimers devoid of CP43 and the water oxidase complex (WOC) could be photoactivated by the addition of Mn^{2+}, Ca^{2+}, Cl^-, and an electron acceptor to assemble an active $Mn_4Ca_1Cl_x$ cluster that produced oxygen under illumination. Fig. 1*A* shows a typical trace of reconstituted, flash-induced oxygen evolution recorded by using CP47RC dimers at a concentration of 10 μM RCs, 40 μM $MnCl_2$, and 80 mM $CaCl_2$ with a 3-s dark interval (t_{dark}) between the light flashes. It was essential to use a programmed light-pulse sequence with low initial light flux; the first flash had a duration of 5 ms and each subsequent flash was lengthened 0.5 ms longer so that the duration of the final (400th) flash was 205 ms. If the flash duration or intensity was increased, the yield of oxygen per flash of photoactivated centers was reduced because of irreversible light-induced photoinhibition of the reaction center (data not shown). After 90 s of dark, the sample was subjected to a second illumination cycle of 400 flashes (Fig. 2*A*, trace II) but with the flash length increased by 1 ms per flash to reach a higher quantum dose at the end of the run. As can be seen in Fig. 2*A* (trace II), once activated, the complexes were able to use these higher light doses and increase the overall yield in oxygen production as compared with the first cycle of illumination. Oxygen production was strictly dependent on the concentrations of manganese and calcium, and the maximal oxygen evolution under the conditions used for the traces shown in Fig. 2*A* was, on average, 5.3% of the oxygen yield of photoactivated apo-WOC-PSII membranes based on RC concentration.

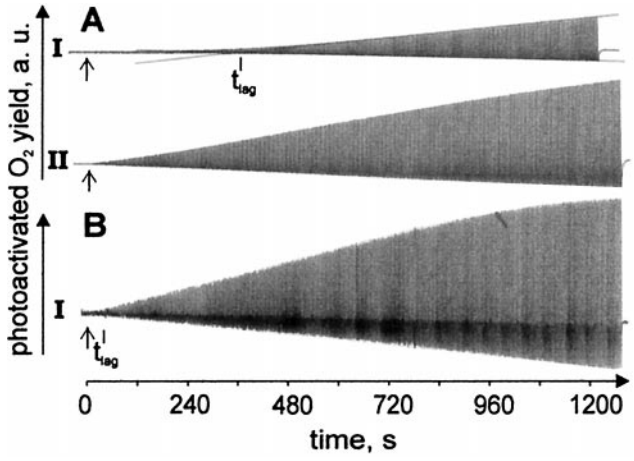

Fig. 2. Photoactivation of CP47RC dimers as measured by flash-induced oxygen evolution. (*A*) Solution contained 40 μM $MnCl_2$, 80 mM $CaCl_2$, protein equivalent to 10 μM RCs, and 0.8 mM ferricyanide. (*B*) As in *A* plus 1 mM DCBQ. Each trace represents illumination by 400 flashes of increasing duration and spaced by 3-s dark time. (I) First illumination, flash length increasing linearly from 5 ms to 205 ms (*A*) or from 5 ms to 405 ms (*B*). (*II*) Second illumination, flash length increasing linearly from 5 ms to 405 ms. The lag time parameter (t_{lag}) was determined by extrapolating the slope of the flash-induced yield to the baseline as indicated in the figure. The maximal oxygen yield refers to the value estimated at the end of the second cycle of illumination (i.e., with 405-ms flash length).

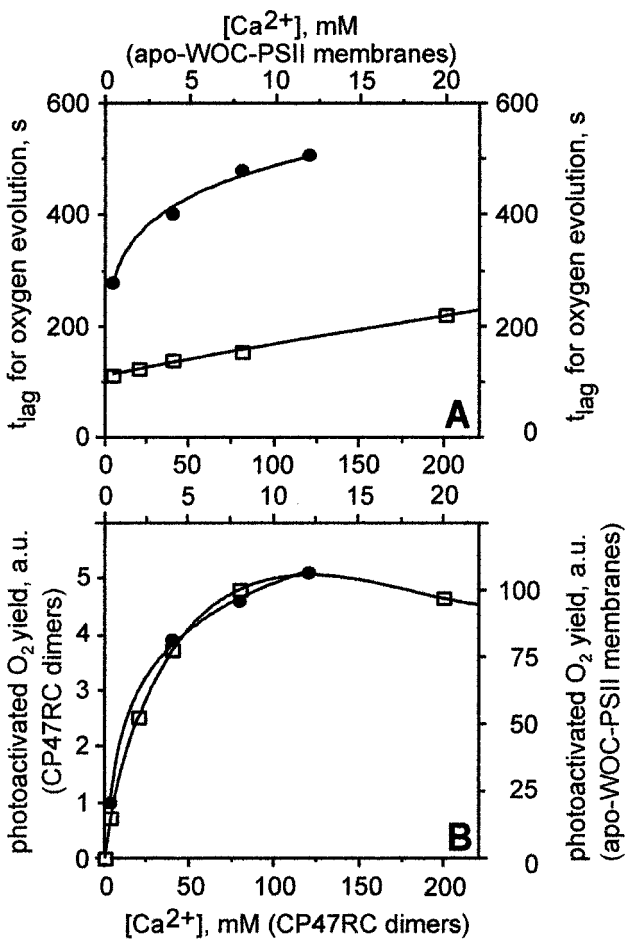

Fig. 3. Dependence of the t_{lag} for photoactivation (*A*) and maximal oxygen yield (*B*) of activated centers of CP47RC dimers (●) and apo-WOC-PSII membranes (□) on $CaCl_2$ concentration. For CP47RC dimers, measurements were conducted on samples in buffer containing 40 μM $MnCl_2$, protein equivalent to 10 μM RCs, and 0.8 mM ferricyanide. Light conditions are as shown in Fig. 2. The t_{lag} was estimated by using data from the first illumination cycle (see Fig. 2*A*), whereas the maximal oxygen evolution refers to the maximal yield at the end of a second illumination cycle. Data for apo-WOC-PSII membranes were taken from ref. 22.

Although the CP47RC dimers were shown to contain some Q_A (30), ferricyanide was not the optimal electron acceptor. This conclusion comes from using quinone derivatives as electron acceptors such as dichloro-benzoquinone (DCBQ) and PPBQ, which, although serving as better acceptors than ferricyanide, also are absorbed in the membrane of the oxygen electrode, giving rise to artificial signals upon illumination. It was found, however, by using a fresh membrane and 1 mM DCBQ together with 0.8 mM ferricyanide that the maximal oxygen yield of the CP47RC dimers could be increased further by 60%, giving an 8.5% yield compared with apo-WOC-PSII membranes (see Fig. 2*B*). Also, the presence of DCBQ supplementing the ferricyanide allowed us to use a stronger illumination regime for photoactivation (first illumination cycle), which usually was applied only for the second cycle. In so doing, it produced an acceleration of photoactivation (as shown by the slope depicted in Fig. 2*A*) and a 6-fold reduction of the lag time of oxygen production, i.e., the time between the first flash given and the onset of oxygen evolution, t_{lag} (compare Fig. 2 *A* and *B*). This result clearly demonstrates the limitations of the CP47RC complex on the acceptor side and has important consequences especially during the first series of light flashes when there is a high probability of photoinhibition occurring because of recombination reactions leading to P680 triplets and singlet oxygen production (34–37). Higher ferricyanide concentrations did not compensate for the quinone effect, and above 0.8 mM ferricyanide, the maximal yield of oxygen production actually was depressed (data not shown).

Although the dimeric CP47RC complex was able to be photoactivated and produced significant amounts of oxygen, the photoactivation that occurred was much slower than in apo-WOC-PSII membranes over a range of Ca^{2+} to RC stoichiometries, as depicted in Fig. 3*A*. For example, t_{lag} was, on average, about 400 s for the CP47RC dimers and about 180 s for apo-WOC-PSII membranes under identical conditions as used for the experiment of Fig. 2*A*. Moreover, CP47RC dimers exhibited a more rapid increase in the lag time with increasing calcium concentration compared with PSII membranes (Fig. 3*A*). This effect is attributed to enhanced competition for binding of Ca^{2+} at the high-affinity Mn^{2+}-binding site, owing to poorer discrimination between these cations and, thereby, slowing the formation of IM_1. This competition is considerably weaker but nonetheless observable in apo-WOC-PSII membranes (23).

As with PSII-enriched membranes, the maximal oxygen yield from CP47RC dimers after completion of photoactivation increased monotonically with Ca^{2+} concentration approaching saturation at 120 mM of Ca^{2+} in the reaction mixture (Fig. 3*B*). This yields an apparent Michaelis constant (K_M) of 12–20 mM. These data are compared directly in Fig. 3*B* with the calcium requirement observed for photoactivation of apo-WOC-PSII membranes, which previously was found to exhibit a K_M of 1.5 mM (23).

Fig. 4 shows the dependence on the manganese concentration of the lag time for photoactivation and oxygen yield after 400 flashes. The lag time decreased smoothly with increasing Mn^{2+} concentration from about 770 s at 0.5 Mn^{2+}/RC to 290 s at 12 Mn^{2+}/RC, about 2-fold slower than PSII membranes (Fig. 4*A*). This trend approaches that observed with apo-WOC-PSII mem-

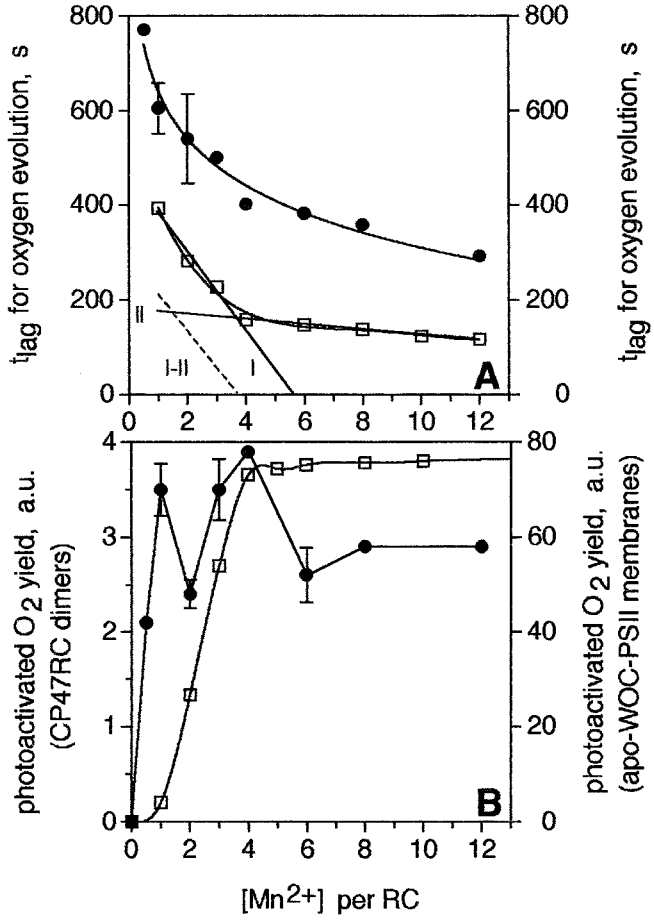

Fig. 4. Dependence of the t_{lag} for photoactivation (*A*) and maximal oxygen yield (*B*) of activated centers of CP47RC dimers (●) and apo-WOC-PSII membranes (□) on $MnCl_2$ concentration. CP47RC dimers were measured in buffer containing 80 mM $CaCl_2$, protein equivalent to 10 μM RCs, and 0.8 mM ferricyanide. Light conditions are as shown in Fig. 2. The t_{lag} and maximal oxygen evolution were determined as in Fig. 3. Bars = mean values ± SD of at least three independent measurements carried out by using two different sample preparations. The t_{lag} data for PSII membranes were fitted to two first-order processes in Mn^{2+} concentration ($t_{lag} = a_i[Mn/RC] + b_i$; i = 1, 2; lines I and II). The dashed line equals I-II.

branes, where the shorter lag time exhibits a distinctly biphasic dependence on Mn^{2+} concentration, with strong acceleration by the first 4 Mn^{2+} and a much weaker acceleration by the next 8 Mn^{2+} added to the solution (21). The t_{lag} data in Fig. 4*A* for PSII membranes were fitted to two first-order processes in Mn^{2+} concentration ($t_{lag} = a_i[Mn/RC] + b_i$; i = 1, 2; lines I and II in Fig. 4*A*). The X intercept for the initial first-order, Mn^{2+}-dependent kinetic phase (line I-II in Fig. 4*A*) is equal to 3.7, which corresponds to the minimal Mn^{2+}/RC stoichiometry required for reactivation of O_2 evolution. In Scheme 1, this stoichiometry refers to one Mn^{2+} in step k_1 (formation of IM_1) plus three kinetically unobserved Mn^{2+} required in all subsequent steps (23). The lag time data for CP47RC dimers did not fit so well to this biphasic model, owing to greater heterogeneity, but approximately the same Mn^{2+}/RC stoichiometry appears to be required.

As shown in Fig. 4*B*, CP47RCs exhibit an unexpected Mn^{2+} concentration dependence of the photoactivation yield, with maxima observed at 1 and 4 Mn^{2+}/RC, a minimum at 2, and a constant but reduced activity (75% of maximum) between 6 and 12 Mn/RC. This curious behavior was checked carefully for

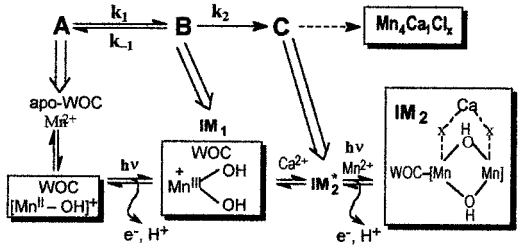

Scheme 1. Model of the kinetic steps involved in the assembly of the WOC by photoactivation (24).

reproducibility by using two different sample preparations and saturating concentrations of calcium. The origin of this bimodal dependence on Mn concentration was not investigated further, but indicates a new type of behavior not seen previously. It stands in marked contrast to the O_2 yield in PSII membranes (Fig. 4*B*), which, in the presence of saturating levels of calcium, increases smoothly, saturates at 4 Mn/RC, and remains constant from 4 to 12 Mn/RC before decreasing above 20 Mn/RC (21). The latter, simple behavior previously was attributed to cooperative uptake of Mn^{2+} that is limited to 4 Mn^{2+} by the presence of calcium during assembly of each active WOC.

Because the time for photoactivation was significantly slower for the CP47RC dimers than with PSII membranes, we determined the constant (k_2, Scheme 1) for the rate-limiting step for the single-exponential process between IM_1 and IM_2 according to the minimal kinetic model of Zaltsman *et al.* (23). Using the conditions described in Fig. 2*A* to minimize the effect of photoinhibition and normalizing the oxygen yield to a constant flash length (by dividing the O_2 yield by the duration of the flash), k_2 was calculated to be 0.54×10^{-3}/s, about 10 times less than in PSII membranes. This apparent rate constant provides a direct comparison of the assembly efficiency of CP47RCs vs. PSII membranes under subsaturating illumination. To take account of the different probabilities for light absorption (cross-sections), we further normalized k_2 by the Chl/RC stoichiometries in CP47RC (21 Chl/RC) and PSII membranes (200–250 Chl/RC). This gives a normalized value of k_2/Chl = 2.6×10^{-5}/s, which is indistinguishable from the value of k_2/Chl = $2.3–2.9 \times 10^{-5}$/s reported previously for PSII membranes (23).

The dependence of photoactivation on the interpulse dark period was investigated. Fig. 5 shows that by increasing the dark time between flashes in the CP47RC dimers, the maximum O_2 yield increases and reaches a maximum near a 5-s dark period, whereas both longer (7-s) and shorter (3-s) periods lead to substantially smaller O_2 yields. The 5-s optimum dark period contrasts with the 3-s optimum for apo-WOC-PSII membranes, indicating either a slower dark step(s) or faster deactivation of the light-induced intermediates during or after the rate-limiting step in assembly. Using a t_{dark} of 5 s, the maximal oxygen yield of the CP47RC dimers was increased further by a factor of 2.1 in comparison with a 3-s dark time, so that under the best conditions we observed (i.e., 5-s dark interval and using DCBQ as an additional electron acceptor and ferricyanide) that the oxygen yield/RC reached about 18% of that of PSII membranes. We anticipate that more thorough examination of these parameters could increase the yield even further.

Fig. 5 also illustrates the sensitive balance between photoactivation and photoinhibition. The relative yield of O_2 produced by a single flash at the end of two consecutive illumination cycles (400 flashes each) applied to a fully photoactivated sample was found to decrease when using dark intervals between flashes shorter than 5 s. A 10% loss because of photoinhibition was found after the third of three such cycles. When the flash intensity was increased five times, complete photoinhibition

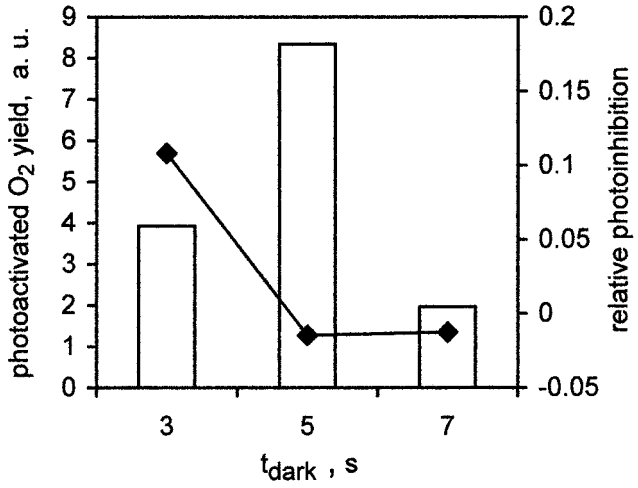

Fig. 5. Maximal oxygen evolution rate of photoactivated CP47RC dimers (bars) and relative photoinhibition (◆) vs. dark time between the flashes. Reaction mixture contained 40 μM $MnCl_2$, 80 mM $CaCl_2$, protein equivalent to 10 μM RCs, and 0.8 mM ferricyanide. Photoinhibition was calculated as the relative loss of maximal oxygen evolution on the final flash of 405 ms of a third cycle of illumination with the yield on the last flash of the second cycle (both cycles measured under conditions identical with those of Fig. 2*A*, trace II).

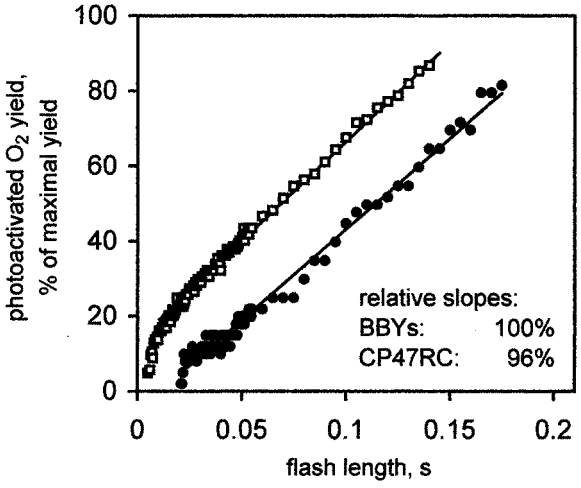

Fig. 6. Initial slopes of the oxygen yield vs. light-dose curves for PSII-enriched membranes (□) and CP47RC dimers (●). Experiments were carried out as in Fig. 2, except that for the CP47RC dimers, a t_{dark} of 5 s was used. Samples were photoactivated in a first cycle of illumination, and the values plotted reflect the oxygen evolution yields during a second cycle. To account for the fact that only part of the CP47RC dimers could be photoactivated, the values were normalized to the maximal oxygen yield of the samples measured in continuous light. Because of the differences in absorption cross-sections, the data were standardized further to identical antenna size. *Inset* gives the values for the slopes calculated by linear regression.

occurred with CP47RC dimers. No such photoinhibition was observed under similar conditions with reactivated apo-WOC-PSII membranes (data not shown). Thus, reactivated CP47RCs are intrinsically more susceptible to photoinhibition of O_2 evolution than are reactivated PSII membranes.

An estimate of the quantum efficiency of photoactivated CP47RC complexes for water oxidation is given by the data in Fig. 6, which compares fully photoactivated PSII membranes and CP47RC dimers in a plot of normalized oxygen yield vs. flash length. Each data set was normalized by division by a constant equal to the maximal oxygen yield of the samples in saturating continuous light of 800 mW/cm^2. In the plot, the relative yields depict the activity of only photoactivated centers and, therefore, are independent of the amount of nonactivatable centers. The slopes reflect the relative quantum efficiencies of the activated centers. Because the absorption cross-section of CP47RC dimer is much smaller than that of PSII membranes because of their smaller antenna size, we normalized further by using Chl/RC stoichiometries of 250 for PSII membranes and 21 for CP47RC dimers. The slopes of these curves then were calculated by using linear regression analysis. The slopes indicate that the photoactivated WOC clusters in the CP47RC dimers are about 96% as efficient as those in the PSII membranes under nonsaturating light conditions.

To get further information about the minimal unit needed for photoactivation, CP47RC monomers also were tested. Despite the lack of quinone in the CP47RC monomers (30), reactivation of oxygen evolution also was achieved by using ferricyanide as an acceptor, although more problems with photoinhibition were encountered. Photoactivation of CP47RC monomers was obtained by using 4 μM Mn^{2+} and 8 mM Ca^{2+} per μM RC, a t_{dark} of 5 s, and shorter flash lengths during the first illumination cycle compared with the light regime used for dimers (5–105 ms with 0.25-ms steps during the first 400 flashes). Little attempt was made to find the optimal conditions for photoactivation of monomers. However, by activating the monomers using the conditions above, a maximal oxygen evolution yield of 40% of the dimers could be reached, measured under the same conditions.

Conclusions

We have shown that it is possible to reconstitute the $Mn_4Ca_1Cl_x$ cluster into the isolated CP47RC subcore complex and restore oxygen evolution. Before these observations, there have been no reports to suggest that a subcomplex of PSII depleted of CP43 could carry out the water oxidation reaction. To date, it has been believed that the minimal unit for the water oxidase activity of PSII is the core complex composed of the D1 and D2 reaction center proteins, CP47 and CP43 inner antenna proteins, and a number of low-molecular-weight proteins including the α- and β-subunits of cytochrome b_{559} (26). The dimeric form of CP47RC was found to be more amenable to photoactivation of the Mn cluster although the CP47RC monomer also showed some capacity to catalyze water oxidation by using similar reconstitution procedures. In the case of the dimer, the presence of bound plastoquinone in the subcomplex (30) helps to reduce the frequency of recombination reactions (31), which, in turn, not only aids electron donation to the added ferricyanide acceptor, but also lowers the yield of P680 triplet formation. This triplet is not quenched by the β-carotene in the RC but, instead, interacts with oxygen to form singlet oxygen (34). The formation of singlet oxygen and possibly other processes resulting from inefficient electron supply on the donor side may render the PSII RC highly sensitive to photoinduced damage. Thus, the success of the reconstitution experiments with the CP47RC subcomplexes is a balance between the reactivation process and the detrimental effects of photoinduced damage. Also to be taken into consideration is that we used Tris washing at pH 9.0 to remove the extrinsic proteins during the isolation procedure. This treatment was shown earlier to decrease the ability of PSII-enriched membranes or cores to restore a fully functional oxygen-evolving complex (26). Nevertheless, with the best conditions that we found (with DCBQ and ferricyanide present, t_{dark} of 5 s and use of short, red wavelength light pulses at early stages of assembly), we obtained an overall O_2 yield that was about 18% of that observed with reactivated, PSII-enriched membranes using the same light intensity. This level of oxygen evolution

recorded is sufficiently high to dismiss the possibility of contamination by core complexes containing CP43, because the level of this protein was 0.3% in dimers and undetectable in CP47RC monomers.

The Mn^{2+} requirement for stimulation of the first step of photoactivation and the total Mn^{2+} stoichiometry (4 Mn^{2+}/RC) appear to be approximately the same for PSII membranes and CP47RC dimers (Fig. 4). The affinity for Ca^{2+} during photoactivation is about 10 times lower in CP47RC dimers compared with PSII membranes as determined by the K_M. However, the rate constant for the slowest step in photoactivation, when normalized for the different light absorption probabilities (k_2/Chl), is found to be indistinguishable from the apo-WOC-PSII membranes. Thus, the CP47RC dimers appear to be a fully native-like unit from the point of early photoactivation steps. The relative quantum efficiency for O_2 production by activated CP47RC subcores was calculated to be 96% of that observed with the more native-like PSII membranes (Fig. 6) after optimization of the various parameters and under subsaturating light intensities and longer dark interval between flashes. Thus, from the point of view of both O_2 evolution yield and photoactivation kinetics, the CP47RC complex behaves very much like a PSII membrane with smaller absorption cross-section and lower affinity for calcium. The main differences between these complexes are the greatly increased susceptibility to photoinhibition (Fig. 5), slower dark assembly step(s) after the rate-limiting k_2 step (Fig. 5), and the unusual oscillation in O_2 yield with Mn^{2+} concentration (Fig. 4).

From our results we conclude that CP43 is not required for the water oxidase activity of PSII, although mutational studies have demonstrated its involvement in normal PSII assembly and function *in vivo* (38–40). In particular, deletion of the gene encoding CP43 resulted in the assembly of a low level of a CP47RC complex unable to evolve oxygen but showing light-driven electron transfer from Y_Z to Q_A (29). In contrast, the deletion of the genes encoding CP47, D1, or D2 proteins resulted in no PSII assembly (1, 38). These findings, therefore, emphasized that CP43 is less critical for PSII, and our results now extend this conclusion to the assembly of the Mn_4 cluster and the water-splitting reaction. Thus, it can be concluded that the minimal unit for catalyzing water splitting is not the PSII core complex containing CP43 as previously thought, but a smaller unit. Here we have demonstrated that the CP47RC complex is one such minimal unit. Whether the Mn cluster can be reconstituted and activated in a complex devoid of CP47 awaits further investigations.

This work was supported by the Biotechnology and Biological Sciences Research Council (J.B.) and by U.S. Department of Agriculture Grant 96–35306-3433/National Institutes of Health Grant GM 39932 (C.D.). S.E.'s involvement in the project was within the context of a joint supervision between J.B. and Professor Bertil Andersson, Stockholm.

1. Debus, R. J. (1992) *Biochim. Biophys. Acta* **1102,** 269–352.
2. Hankamer, B., Boekema, E. & Barber, J. (1996) *Annu. Rev. Plant Physiol. Mol. Biol.* **48,** 641–671.
3. Diner, B. A. & Babcock, G. T. (1996) in *Oxygenic Photosynthesis: The Light Reactions*, eds. Ort, D. R. & Yocum, C. F. (Kluwer, Dordrecht, The Netherlands), pp. 213–247.
4. Britt, R. D. (1996) in *Oxygenic Photosynthesis: The Light Reactions*, eds. Ort, D. R. & Yocum, C. F. (Kluwer, Dordrecht, The Netherlands), pp. 137–159.
5. Diner, B. A. (1998) *Methods Enzymol.* **297,** 337–360.
6. Nanba, O. & Satoh, K. (1987) *Proc. Natl. Acad. Sci. USA* **84,** 109–112.
7. Metz, J. G., Nixon, P. J., Rögner, M., Brudvig, G. W. & Diner, B. A. *Biochemistry* **28,** 6960–6969.
8. Nixon, P. & Diner, B. A. (1992) *Biochemistry* **31,** 942–948.
9. Chu, H. A., Nguyen, A. P. & Debus, R. J. (1994) *Biochemistry* **24,** 6137–6149.
10. Chu, H. A., Nguyen A. P. & Debus R. J. (1994) *Biochemistry* **24,** 6150–6157.
11. Wu, J., Masri, N., Lee, W., Frankel, L. K. & Bricker, T. M. (1999) *Plant Mol. Biol.* **39,** 381–386.
12. Knoepfle, N., Bricker, T. M. & Putman-Evans, C. (1999) *Biochemistry* **38,** 1582–1588.
13. Brudvig, G. W. & Crabtree, R. H. (1989) *Prog. Inorganic Chem.* **37,** 99–142.
14. Yachandra, V. K., Sauer, K. & Klein, M. P. (1996) *Chem. Rev.* **96,** 2927–2950.
15. Rüttinger, W. & Dismukes, G. C. (1997) *Chem. Rev.* **97,** 1–24.
16. Bricker, T. M. & Frankel, L. K. (1998) *Photosynth. Res.* **56,** 157–173.
17. Cheniae, G. M. & Martin, I. F. (1971) *Biochim. Biophys. Acta.* **253,** 167–181.
18. Ono, T. & Inoue, Y. (1983) *Biochim. Biophys. Acta* **723,** 191–201.
19. Tamura, N. & Cheniae, G. (1987) *Biochim. Biophys. Acta* **890,** 179–194.
20. Tamura, N. & Cheniae, G. M. (1986) *FEBS Lett.* **200,** 231–236.
21. Ananyev, G. M. & Dismukes, G. C. (1996) *Biochemistry* **35,** 4102–4109.
22. Ananyev, G. M. & Dismukes, G. C. (1996) *Biochemistry* **35,** 14608–14617.
23. Zaltsman, L., Ananyev, G. M., Bruntrager, E. & Dismukes, G. C. (1997) *Biochemistry* **36,** 8914–8922.
24. Ananyev, G. M., Murphy, A., Abe, Y. & Dismukes, G. C. (1999) *Biochemistry* **38,** 7200–7209.
25. Ananyev, G. & Dismukes, G. C. (1995) in *Photosynthesis: From Light to Biosphere*, ed. Mathis, P. (Kluwer, Dordrecht, The Netherlands), Vol. 2, pp. 431–434.
26. Tamura, N., Kamachi, H., Hokari, N., Masumoto, H. & Inoue, H. (1991) *Biochim. Biophys. Acta* **1060,** 51–58.
27. Oku, T. & Tomita, G. (1976) *Physiol. Plant.* **38,** 181–185.
28. Rova, E. M., McEwen, B., Fredriksson, P. O. & Styring, S. (1996) *J. Biol. Chem.* **271,** 28918–28924.
29. Rögner, M., Chisholm, D. A. & Diner, B. A. (1991) *Biochemistry* **30,** 5387–5395.
30. Zheleva, D., Sharma, J., Panica, M., Morris, H. & Barber, J. (1998) *J. Biol. Chem.* **272,** 16122–16127.
31. Bianchetti, M., Zheleva, D., Deak, Z., Zharmuhamedov, S., Klimov, V., Nugent, J., Vass, I. & Barber, J. (1998) *J. Biol. Chem.* **273,** 16128–16133.
32. Berthold, D. A., Babcock, G. T. & Yocum, C. F. (1981) *FEBS Lett.* **134,** 231–234.
33. Büchel, C., Morris, E. & Barber, J. (1998) in *Photosynthesis: Mechanisms and Effects*, ed. Garab, G. (Kluwer, Dordrecht, The Netherlands), pp. 953–956.
34. Durrant, J. R., Giorgi, L. B., Barber, J., Klug, D. R. & Porter, G. (1990) *Biochim. Biophys. Acta* **1017,** 167–175.
35. Vass, I. & Styring, S. (1992) *Biochemistry* **31,** 5957–5963.
36. Seibert, M. (1993) in *The Photosynthetic Reaction Center*, eds. Deisenhofer, J. & Norris, J. R. (Academic, San Diego), pp. 319–356.
37. Krieger, A., Rutherford, A. W., Vass, I. & Hideg, E. (1998) *Biochemistry* **37,** 16262–16269.
38. Vermaas, W. F. J., Ikeuchi, M. & Inoue, Y. (1988) *Photosynth. Res.* **17,** 97–113.
39. Kuhn, M. G. & Vermaas, W. (1993) *Plant Mol. Biol.* **23,** 123–133.
40. Manna, P. & Vermaas, W. (1997) *Eur. J. Biochem.* **247,** 666–672.